P. Schroth, R. Engel, F.S. Cox, Middletown, Ohio

ON THE LABORATORY TESTING OF INSULATING FIBER PRODUCTS

Introduction

The increase in energy costs over the last decade has necessitated more widespread use of insulation in the various heating furnaces throughout the steel industry. Principally, two types of insulating refractories are utilized, namely fired brick or castables on the one hand and fiber products in numerous shapes and forms on the other hand. Of the two material types, refractory fibers are the more recent development. While fibers were in existence in the early 1970's when the first quantum jump in energy prices occurred, experience with fibers was limited at that time and was purely empirical.

In the last several years refractory fiber usage has increased markedly. From 1975 through 1980, fiber product application grew at a 20% annual rate. For the years until 1985 this rate of increase is expected to slow to about 15% per year, with the growth potential shifting to high temperature fibers. It is obvious that these opportunities have created more suppliers and a greater variety of products. For the user of refractory fiber products, this meant the need to discriminate between a greater number of products for the same as well as different applications.

Technical Background

In the absence of specific test procedures and standards, early evaluations of fibers relied entirely on empirical data and performance results. Field experience had shown that refractory fibers did an excellent job as low temperature insulation on the cold face of wall and/or roof systems. However, this was not necessarily true in those cases where the refractory fibers were used for hot face veneering applications, particularly if temperatures were near their use limit. This could even be observed in instances where flame impingement and/or contamination of the atmosphere were not essential variables. All these factors supported the view that laboratory tests for fiber products were imperative in the long run.

At Armco, many hot face installations failed, due to shrinkage of fiber products which had been deemed quite suitable for the given application and temperature. It must be pointed out that this occurred mainly in those cases where fiber modules were used and furnace temperatures were typically near the use limits of the materials. While all furnaces which had been lined or veneered with fiber insulation showed substantial operating savings in fuel consumption, furnace availability remained often unsatisfactory as many maintenance outages were caused by fiber shrinkage and subsequent anchor and/or shell deterioration and failure.

These experiences demonstrated the need for a laboratory type fiber shrinkage test. It was not expected that an ASTM Standard Test on Fiber Shrinkage would be introduced any time soon. Therefore Armco Refractory Research began to develop a laboratory test which was designed to discriminate between the shrinkage behavior of different refractory fiber products. As this was exploratory work, it was decided to utilize equipment that was already available at the laboratories. As a result an all purpose gas fired kiln was used for early test development work. It can be seen in Figure 1.

Exploratory Fiber Testing

The original method that was used to generate shrinkage data on fiber blanket insulation was a modified reheat test. The samples were cut from blankets measuring 230mm x 115mm x the thickness of the blanket (approximately 25mm). The test specimens were then put between two 1650°C class insulating firebrick. The actual thickness of the blanket was measured in four places using a rule. The samples were located in the kiln as shown in Figures 2 and 3. The side baffles were intended to block any direct flame impingement on the samples. Employing the center baffle as shown, it was intended to introduce a thermal gradient through the sample similar to what would be experienced in service. Another simulation of field conditions, compression of the material, was accomplished by placing the insulating firebrick on top of the fiber sample.

The kiln was then taken to a specified temperature in two hours and held for four hours. After cooling, all samples were remeasured and shrinkage calculated. This test was conducted for seven or eight temperature ranges and several reproducibility runs were made. The data obtained from the various runs to different temperatures were plotted to generate a continuous shrinkage curve. The test set-up indeed produced shrinkage rates which varied for the "hot face" and "cold face" locations. Unfortunately, reproducibility was so poor that it did not seem promising to further pursue test development with this equipment.

Presently Used Fiber Testing Procedure

Equipment

As a result of this early exploratory work, another attempt to develop fiber shrinkage data was made, utilizing again a piece of existing equipment. The apparatus used to measure shrinkage values for the fibers in this particular study was a Harrop TDA-VI-6 Creep Furnace. It is shown in Figure 4. The furnace was originally designed to measure the creep of materials while being subjected to

a constant compressive load of up to about 1,400 kPa on a sample of 50mm x 50mm in cross section. The unit is comprised of two primary electrical systems, the temperature control and the dilation system. The temperature control system consists of a programer, two controllers, a 440V single phase, 100 Amp power supply and six channels of a twelve channel recorder. See Figure 5. To operate this system a line representing the desired rate of temperature rise and/or other functions is drawn on the programer chart. The programer feeds the information into the temperature controllers that increase or decrease an electrical signal to the SCR (silicon controlled rectifier) power control which in turn varies the power input to the furnace. The temperature in the furnace is plotted on a strip chart recorder as a function of time.

The dilation measuring system is made up of an electrical/mechanical network which consists of a measuring frame, transducers, ceramic push rods, electrical oscillators and demodulators and the other six channels of the twelve channel recorder. The material to be tested is placed in the furnace directly under a push rod. This rod rests on the sample, extends outside of the furnace and is connected to a transducer core. The furnace is then heated causing a dimensional change in the sample. This change is transmitted to the core of the transducer which provides a voltage output proportional to the amount of displacement. This voltage is received by a signal conditioning system. The output of the signal conditioner is subsequently fed into the recorder and plotted as a function of time and temperature. The transducer and the standard push rod located in the center of the furnace correct for errors caused by dimensional changes of the entire system.

Since all push rods are made of the same material, they all have the same reference point at the same temperature. As the furnace is heated, the push rods, samples and bases expand, causing a deflection in the transducer. The output of the correction transducer is equal to the negative expansion of push rods and bases. The transducer signals are fed into a summing junction where the sample and correction signals are compared. The difference is the actual sample expansion.

The system is considered to be very sensitive to dimensional changes as a function of temperature. It was hoped that it would measure even minor differences in the shrinkage of various fiber materials. While it is realized that one of the desirable parameters, namely the thermal gradient, cannot be introduced into the test set up, another practical factor, compression, can be handled experimentally by the placing of a flat slice and push rod on top of the sample specimen and compressing it simply by their weight.

Test Method

A sample was cut from each test material, which in this case were blankets for the sake of convenience. The samples were approximately 50mm x 50mm by whatever thickness the blanket took when it was compressed by the weight of the alumina slice and push rod. The approximate load was determined to be 1.2 kPa. The sample was sandwiched between the 6mm alumina slice on top and a 25mm base of isopressed alumina at the bottom. This is schematically shown in Figure 6. The push rod was placed on top of the 6mm slice and the original measurement of thickness was made using a rule. An average of four measurements, one on each side, was taken and the sample was placed in the furnace in one of six positions. The sample had to be built up with leveling slices of isopressed alumina so that the same length of push rod was in the furnace for all samples including the correction position. The importance of this requirement cannot be overemphasized. It is also very critical that the push rod be centered on the sample so that shrinkage occurs equally and is not localized on one side.

After all six positions were loaded, the furnace was closed up and the process of zeroing the transducers with the correction channel was begun. After this was accomplished the furnace was switched on and the heat-up commenced. The heat-up schedule was 250°C/hr. to 1500°C. Upon reaching 1500°C the furnace was switched off and allowed to cool overnight. The samples were removed the next day and measured again after they had cooled down to room temperature.

Total shrinkage was then calculated. To determine intermediate temperature shrinkage values, the data points from the temperature dilation chart were evaluated. These were then plotted on a graph to show continuous shrinkage.

Test Results

Eight different insulating fiber materials were tested under the conditions described above. Table I provides the approximate chemical analyses, densities and recommended temperature use limits of the test materials. These are manufacturer supplied data. The shrinkage characteristics for these materials as determined in the Armco Refractories Research laboratories can be found in Table II. An analysis of this test series showed principally three different shrinkage behaviors to exist. The first group is characterized by slight expansion before continuous shrinkage. The second group includes the fibers which also expand somewhat but have an S-shaped shrinkage curve with the inflection point at or near 1000°C. Finally, the third group is comprised of fibers with an almost continuous shrinkage plot.

In the ongoing efforts to develop a fiber shrinkage test it was decided to work only with proto types from each group rather than all the fiber products that had been included in the original test series. As a consequence eleven reproducibility runs were made for one typical fiber from each of the three groups. The results are summarized in Table III for fiber E, Table IV for fiber B and Table V for fiber F and graphically depicted in Figures 7 through 9.

These data were statistically analyzed for standard deviation. The computations can be found in Tables VI, VII and VIII for fibers E, B and F, respectively. The standard deviation is further plotted against temperature for fibers E, B and F in Figures 10 through 12.

It is certainly not surprising that the standard deviation increased with temperature. What is unexpected, however, is its reversal at higher temperatures. No explanation for this observation can be given at the present time. It is impossible to predict whether this test will eventually lead to a viable evaluation procedure for fiber products. The main disadvantage of the test is the high standard deviation on reproducibility runs at elevated temperatures. Its principle advantage is the continuous recording of expansion/shrinkage as a function of temperature. Another strong point in favor of this test arrangement is that it imitates field practiced precompression simply by the way the test sample is arranged. The existence of a plate below and above the test specimen has the additional advantage that the determination of the thickness dimension of the sample can be carried out with reasonable accuracy before and after the test. The introduction of a thermal gradient would be desirable but appears elusive at present. It is primarily hoped that future work will bring about an improvement in high temperature reproducibility. Still, there is insufficient knowledge as to what degree of accuracy and precision should be expected from any fiber test when compared with typical refractory brick test procedures, particularly in light of the known inadequacies in determining the original dimensions of the fiber test sample.

Scanning Electrode Microscope Study

No obvious explanation was readily available for the low temperature expansion and the S-shaped inflection characteristics that had been observed. Therefore, further study of this behavior was warranted so the reasons for it might be understood. A typical fiber blanket from each group was carefully scrutinized under the scanning electron microscope after exposure to temperature. The temperatures chosen went from ambient to 1500°C and a bracketing of the points of inflection was incorporated into the test design. The scanning electron microscope used was an AMR, Model 1000A with an attached energy dispersive system, for qualitative chemical analysis. Fiber blanket samples measuring approximately $1cm^3$ were mounted on

aluminum stubs and carbon coated several times as they were highly unstable in the electron beam. Furthermore, the beam spot size had to be adjusted for each blanket type to minimize charging problems.

Figures 13 and 14 show typical views of fiber B after exposure to different temperatures in air. It should be noted that the fibers themselves did not devitrify, but rather they precipitated mullite crystals in ever increasing numbers up to a temperature of about 1100°C, at which point the rate of increase held approximately constant. The mechanism for the formation of these crystals is thought to consist of the thickening of the fiber with or without concurrent necking until it becomes pear shaped. See Figure 15. This system, due to its mode of formation, would be under internal stresses. For relief thin sheaths of material would peel off, which could easily devitrify to form mullite as seen in Figures 16 and 17. The change in fiber density observed throughout these figures should not be considered real as it was probably brought about by the sample mounting process.

Evidence of fiber mullitization for E composition samples could be found at temperatures as low as 700°C. See Figure 18. Almost no other fiber changes occurred until 1150°C were reached, when complete recrystallization to α-Al_2O_3 of some of the alumina fibers was observed as shown in Figures 19 and 20. There is some evidence to indicate the fusing of fibers is brought about by the devitrification/recrystallization process. This is shown in Figure 21.

Sample F is characterized by the presence of mullite from the as received condition to about 1000°C. At this temperature its concentration peaks. Some indication exists that α-Al_2O_3 is formed already at 500°C, but this mode of recrystallization does not take over until temperatures above 1000°C are reached. See Figure 22. In conjunction with this process, cristobalite can be seen forming in Figure 23. Neither of these two end products ever become very abundant, but rather can be found in discreet pockets. This

was the only sample where any SiO_2 polymorph was observed, although phase relations would predict its presence in all of them.

Pasto and Tennery [1] and Dietrichs, et. al [2] indicate the θ-alumina fibers are polycrystalline and microporous after production and consist mainly of alumina and other unstable aluminas. Microscopic migration of these pores in conjunction with their size increase due to the temperature rise may be a reason for the temporary expansion observed in fibers of Group E and B. The inflection point at 1000°C might be a reflection of the peaking of mullite production although this finding would be in disagreement with Dietrichs, et. al. [2]. No temperatures are given for maximum mullite production in the Olds, et. al. [3] or the Pasto and Tennery [1] articles even though both report its presence as a devitrification product of aluminosilicate fibers.

Summary

The importance of insulating systems and their increased use due to the cost of energy requires laboratory evaluation methods for these materials, particularly for refractory fibers. Attempts have been described to develop a fiber shrinkage test which closely follows field conditions. Continuous expansion/ shrinkage was recorded, however, reproducibility of test results appears not to be fully satisfactory at the present time. Several unresolved problems remain open for further study. It was surprising to see some fibers expand in the lower temperature range. Some fibers shrank continuously, others showed an S-shaped inflection curve. In spite of the use of the scanning electron microscope these phenomena could not be fully explained.

Bibliography

1. A. E. Pasto, V. J. Tennery; Effects of Alternate Fuels Refractory Test Facility (RTF), Test 1, Analysis of Selected Aluminosilicate Refractory Brick, Mortars, and Fibrous Insulations Degraded by Domestic Residual Oil Combustion Products, Oak Ridge National Laboratory, ORNL/TM-6351.
2. P. Dietrichs, W. Krönert, F. Kühn; "Criteria for the Selection of Refractories for Use in Heat Treatment Furnaces", Inter Ceram, 29, p. 99-112, 1980.
3. S. E. Olds, W. C. Miller, J. M. Pallo; "High Temperature Aluminosilicate Fibers Stabilized with Cr_2O_3", American Ceramic Society Bulletin, 59, No. 7, p. 739-741, 1980.

TABLE I: FIBER CHARACTERISTICS

MATERIAL	DENSITY Mg/m^3	TEMPERATURE USE LIMIT °C	CHEMISTRY					
			Al_2O_3	SiO_2	Fe_2O_3	TiO_2	Cr_2O_3	Trace
A	1.49	1425	47.89	51.69	0.04	0.002	0.25	0.13
B	1.12	1315	48.0	51.8	0.04	0.002	-	0.13
C	0.96	1370	40.5	55.0	0.21	-	4.0	0.14
D	-	-	47-52	48-53	-	-	-	-
E	0.96	1540	95.0	5.0	-	-	-	-
F	1.60	1370	55.7	38.7	-	-	-	0.5
G	1.28	1315	48-50	49-51	0.8-1.0	1.0-1.3	-	0.2
H	0.96	1315	47.0	52.8	0.02	0.01	-	0.23

TABLE II: SHRINKAGE CHARACTERISTICS

TEMPERATURE °C / MATERIAL	100	200	300	400	500	600	700	800	900	1000	1100	1200	1300	1400	1500
	PERCENT LINEAR CHANGE														
A	-0-	-0-	-1.0	-1.0	-1.0	-1.5	-5.0	-9.0	-16.5	-43.5	-43.0	-42.0	-42.0	-42.0	-42.0
B	-0-	+1.6	+3.0	+4.0	+4.0	+6.0	+5.0	+3.0	-0-	-32.4	-32.0	-32.0	-36.0	-59.0	-65.0
C	-0-	-1.0	+1.0	-0-	-1.8	-2.8	-4.9	-7.0	-16.1	-34.3	-36.4	-53.2	-60.0	-59.3	-60.0
D	-0-	+3.0	+4.3	+5.7	+5.7	+7.9	+11.4	+15.7	+17.9	+17.9	+14.0	+7.2	-24.3	-30.0	-50.1
E	-0-	+1.9	+1.4	+1.4	+1.6	+2.6	+4.2	+5.3	+4.2	+4.2	+4.2	+1.4	-18.9	-24.2	-31.5
F	-0-	+1.0	-4.0	-6.0	-8.0	-9.0	-9.2	-11.4	-14.0	-24.0	-25.0	-28.5	-35.2	-38.0	-43.0
G	-0-	+4.0	+5.0	+8.0	+10.0	+12.0	+8.0	+8.0	-6.0	-16.0	-16.0	-38.0	-40.0	-42.0	-52.0
H	-0-	+1.6	+1.6	+0.8	-0-	-0-	-1.6	-2.4	-5.0	-26.0	-25.0	-26.0	-32.4	-53.4	-56.0

TABLE III: REPRODUCIBILITY RUNS OF FIBER E

Temperature °C Runs	100	200	300	400	500	600	700	800	900	1000	1100	1200	1300	1400	1500
1	-0-	+2.2%	+2.2%	+3.4%	+4.0%	+6.3%	+7.4%	+7.4%	+7.4%	+7.4%	+5.1%	+2.0%	-6.0%	-20.5%	-27.4%
2	-0-	+2.2%	+2.2%	+2.2%	+2.2%	+4.4%	+5.5%	+7.7%	+4.4%	+3.3%	+2.2%	+2.2%	-7.7%	-19.8%	-27.5%
3	-0-	-0-	-0-	-1.0%	-0-	-0-	-0-	-0-	-1.0%	-2.3%	-4.0%	-7.0%	-15.0%	-21.3%	-27.0%
4	-0-	+2.0%	+2.0%	-0-	+1.0%	+1.7%	+2.5%	+3.3%	+3.3%	+1.0%	+1.0%	-2.5%	-14.1%	-20.0%	-24.9%
5	-0-	+1.5%	+1.5%	+1.5%	+2.4%	+3.1%	+3.7%	+4.6%	+4.9%	+2.7%	+2.7%	-0-	-10.7%	-19.5%	-26.8%
6	-0-	+1.0%	+1.6%	+1.6%	+2.4%	+2.4%	+2.4%	+3.2%	+4.0%	+3.2%	+3.2%	-5.7%	-16.4%	-21.3%	-27.9%
7	-0-	+2.2%	+3.4%	+3.4%	+3.4%	+3.4%	+3.4%	+4.5%	+6.7%	+6.7%	+6.7%	-5.6%	-9.0%	-23.5%	-31.4%
8	-0-	+1.0%	-0-	-0-	-0-	-0-	-0-	+1.0%	+1.0%	+1.0%	-0-	-6.9%	-17.3%	-24.8%	-31.7%
9	-0-	+1.0%	+1.0%	+1.0%	+1.0	+1.0%	+1.8%	+2.7%	+4.0%	+2.7%	+2.7%	-2.7%	-13.5%	-24.3%	-29.8%
10	-0-	+1.0%	+1.0%	+1.0%	+1.0%	+1.0%	+1.9%	+2.5%	+3.8%	+2.5%	+2.5%	-1.3%	-12.6%	-25.2%	-32.2%
11	-0-	+1.5%	+1.5%	+1.5%	+1.5%	+2.5%	+4.0%	+5.0%	+4.0%	+4.0%	+4.0%	+1.0%	-19.0%	-24.5%	-31.5%

TABLE IV: REPRODUCIBILITY RUNS OF FIBER B

Temperature °C Runs	100	200	300	400	500	600	700	800	900	1000	1100	1200	1300	1400	1500
1	-0-	+2.0%	+3.0%	+3.0%	+4.0%	+6.0%	+4.0%	+2.0%	-0-	-32.0%	-32.0%	-32.0%	-36.0%	-59.0%	-65.0%
2	-0-	-0-	-0-	-0-	-0-	-1.0%	-2.0%	-4.0%	-8.5%	-28.0%	-28.0%	-30.0%	-36.0%	-49.0%	-55.0%
3	-0-	+2.5%	+5.0%	+10.0%	+12.5%	+14.0%	+14%	+14.0%	+10.0%	-22.5%	-20.0%	-20.0%	-30.0%	-50.0%	-60.0%
4	-0-	+1.5%	+3.0%	+4.5%	+6.0%	+7.0%	+7.0%	+7.0%	-30.0%	-23.2%	-20.0%	-20.0%	-32.0%	-54.0%	-67.0%
5	-0-	+1.0%	+2.0%	+3.0%	+4.0%	+4.0%	+1.0%	-0-	-4.0%	-30.0%	-30.0%	-30.0%	-40.0%	-56.0%	-63.0%
6	-0-	+1.3%	+2.6%	+4.0%	+5.3%	+5.3%	+2.6%	-0-	-10.5%	-34.0%	-39.0%	-39.0%	-42.0%	-49.0%	-60.0%
7	-0-	+2.0%	+4.5%	+5.5%	+6.5%	+6.5%	+6.5%	+2.0%	-7.0%	-23.0%	-26.5%	-26.4%	-35.2%	-59.0%	-65.0%
8	-0-	+3.2%	+4.0%	+5.6%	+8.0%	+9.6%	+11.2%	+10.0%	+5.6%	-32.4%	-29.2%	-29.2%	-37.3%	-56.7%	-60.0%
9	-0-	+1.6%	+3.2%	+4.0%	+5.6%	+5.6%	+5.6%	+5.6%	-0-	-30.8%	-29.2%	-29.2%	-37.3%	-55.1%	-61.6%
10	-0-	+2.6%	+3.3%	+4.1%	+5.2%	+5.2%	+5.2%	+2.6%	-2.6%	-33.8%	-32.5%	-32.5%	-42.9%	-55.9%	-61.1%
11	-0-	+2.6%	+5.0%	+6.9%	+8.1%	+10.0%	+10.0%	+5.0%	+5.0%	-31.3%	-28.8%	-28.8%	-35.0%	-55.0%	-58.8%

TABLE V: REPRODUCIBILITY RUNS OF FIBER F

Temperature °C / Runs	100	200	300	400	500	600	700	800	900	1000	1100	1200	1300	1400	1500
1	-0-	-0-	+1.0	+1.8	+2.3	+3.5	+4.3	+4.3	+2.4	-4.8	-4.8	-14.4	-35.5	-46.1	-48.2
2	-0-	-0-	+1.3	+1.9	+2.6	+3.8	+5.2	+5.2	+3.9	-3.8	-3.8	-18.1	-37.4	-41.3	-46.4
3	-0-	-0-	-0-	-0-	+0.7	+0.7	+1.0	+1.0	-2.6	-14.3	-14.3	-16.3	-29.9	-46.8	-48.3
4	-0-	-0-	-0-	+0.7	+0.7	+0.7	+1.0	+0.7	-1.5	-12.6	-16.3	-18.5	-33.3	-45.1	-48.2
5	-0-	-0-	-0-	+0.6	+1.0	+1.3	+1.9	+1.9	+0.6	-9.6	-16.0	-17.3	-36.5	-53.1	-53.8
6	-0-	+1.0	+1.0	+1.0	+2.0	+2.5	+3.0	+2.0	-5.0	-11.0	-11.0	-18.0	-44.0	-48.0	-54.0
7	-0-	+1.9	+1.9	+1.0	+1.0	+2.3	+3.7	+3.7	+1.0	-11.2	-11.2	-14.0	-37.2	-44.6	-51.2
8	-0-	+0.8	+0.8	-0-	+0.8	+0.8	-0.8	-0.8	-5.2	-15.0	-15.0	-20.3	-37.5	-45.0	-50.1
9	-0-	-0-	-0-	-0.9	-0-	+0.9	-0.9	-0.9	-4.3	-17.1	-17.1	-20.7	-41.5	-49.4	-51.8
10	-0-	-0-	-0.5	-0.2	-3.5	-3.5	-4.0	-5.0	-7.0	-12.0	-13.5	-16.0	-25.0	-39.0	-44.0
11	-0-	-1.0	-4.0	-6.0	-8.0	-9.0	-10.0	-11.5	-14.0	-24.0	-24.0	-29.0	-35.0	-38.0	-43.0

TABLE VI

Material - Fiber E		
Temp	NOBS	STDEV
100	11	0.00000
200	11	0.69974
300	11	0.99243
400	11	1.36535
500	11	1.29214
600	11	1.91330
700	11	2.20240
800	11	2.37758
900	11	2.32692
1000	11	2.65785
1100	11	2.79073
1200	11	3.48840
1300	11	4.12053
1400	11	2.22547
1500	11	2.48549

TABLE VII

Material - Fiber B		
Temp	NOBS	STDEV
100	11	0.00000
200	11	0.89707
300	11	1.44656
400	11	2.52248
500	11	3.10067
600	11	3.80796
700	11	4.62143
800	11	5.18980
900	11	6.31795
1000	11	4.36642
1100	11	5.38802
1200	11	5.40187
1300	11	3.88896
1400	11	3.62080
1500	11	3.36838

TABLE VIII

Material - Fiber F		
Temp	NOBS	STDEV
100	11	0.00000
200	11	0.74748
300	11	1.54872
400	11	2.82199
500	11	3.09686
600	11	3.66259
700	11	4.30986
800	11	4.76432
900	11	5.05486
1000	11	5.56856
1100	11	5.66838
1200	11	4.10191
1300	11	5.15722
1400	11	4.43962
1500	11	3.65630

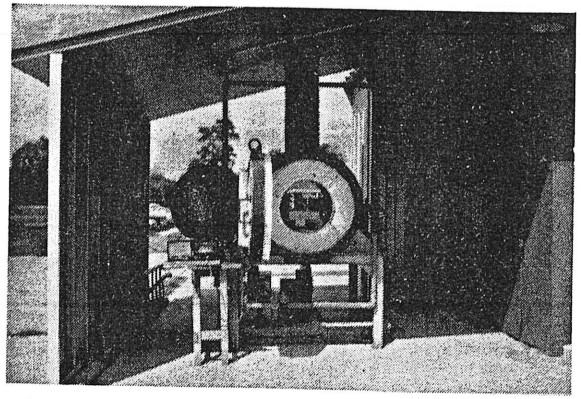

Fig. 1: Gas Fired All-Purpose Kiln

Reheat Set-up For Insulating Fiber Blankets

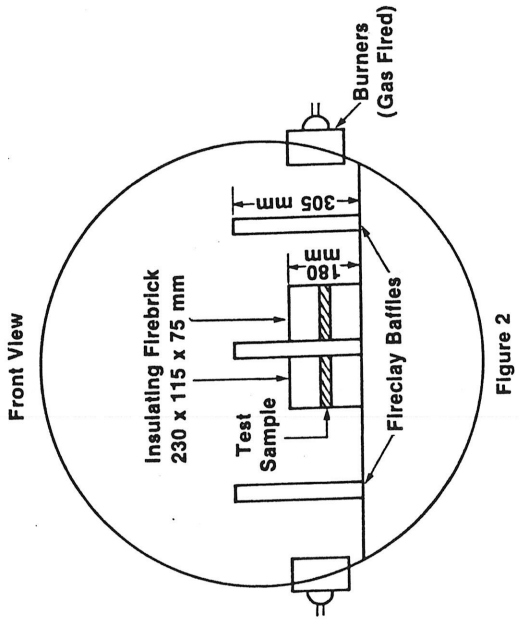

Figure 2

Reheat Set-up For Insulating Fiber Blankets

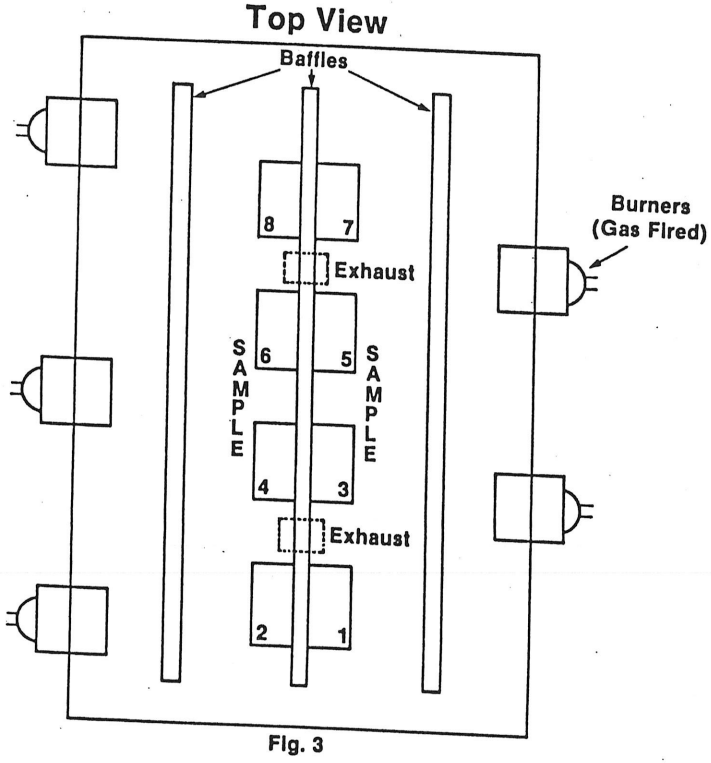

Fig. 3

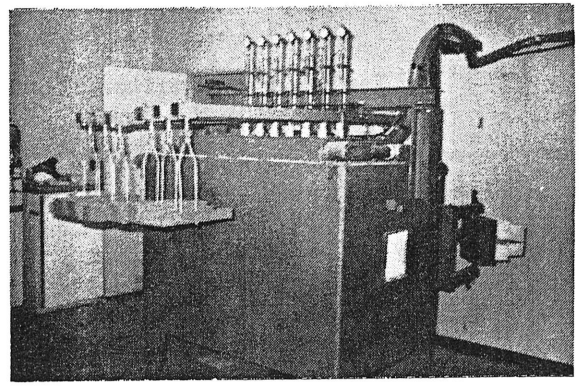

Fig. 4: Harrop TDA-VI-6 Creep Furnace

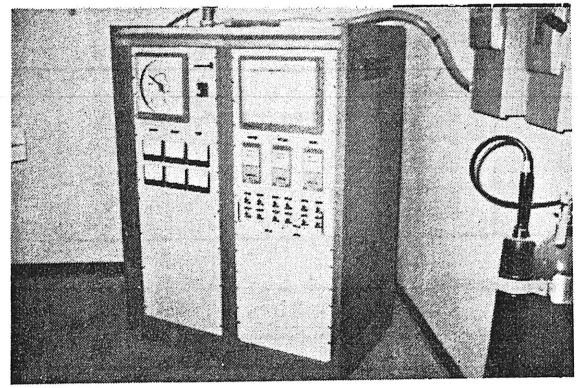

Fig. 5: Control Cabinet for Harrop Creep Furnace

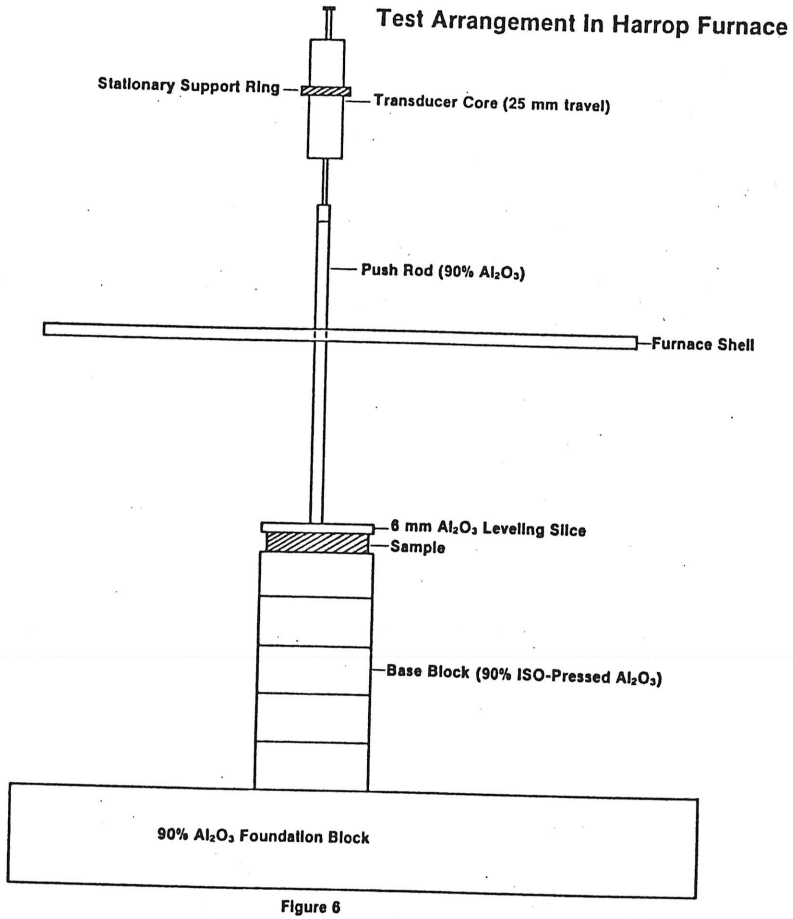

Figure 6

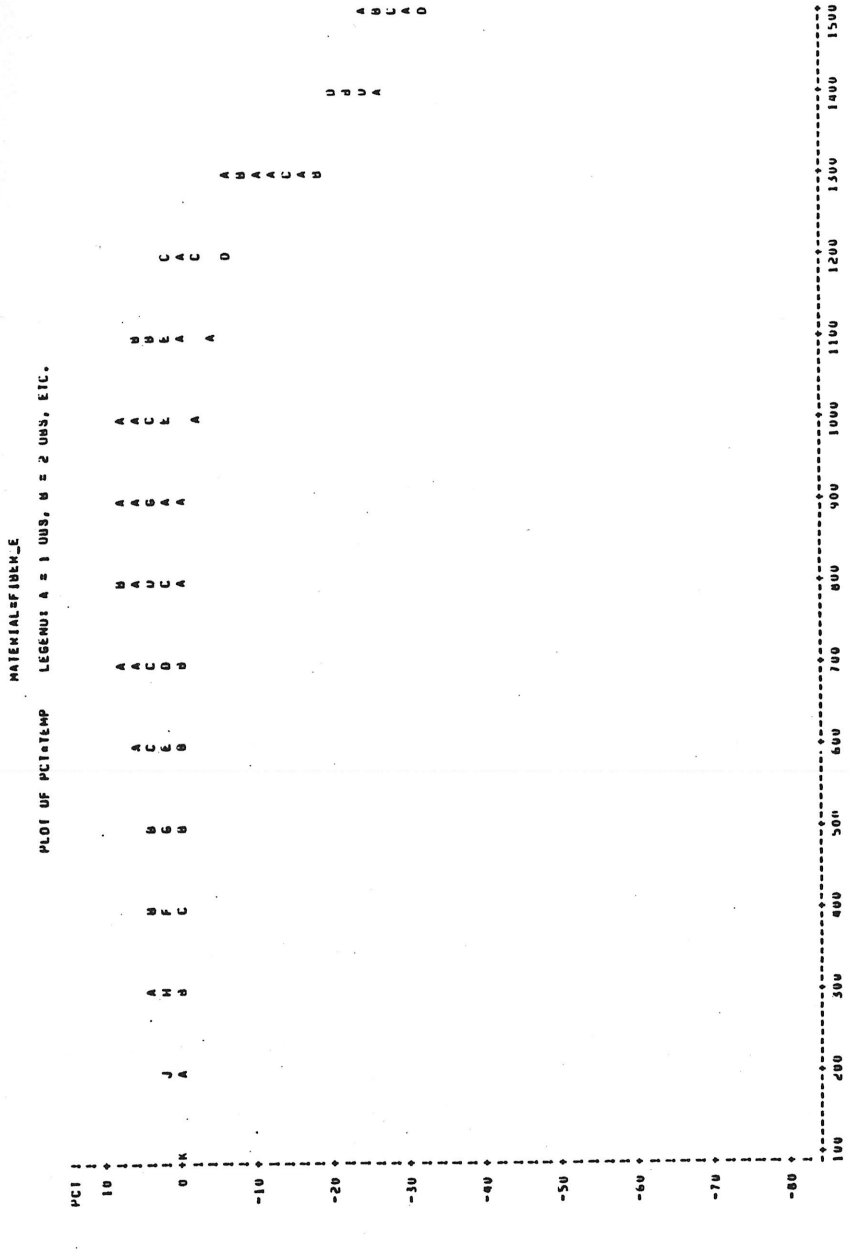

Figure 7

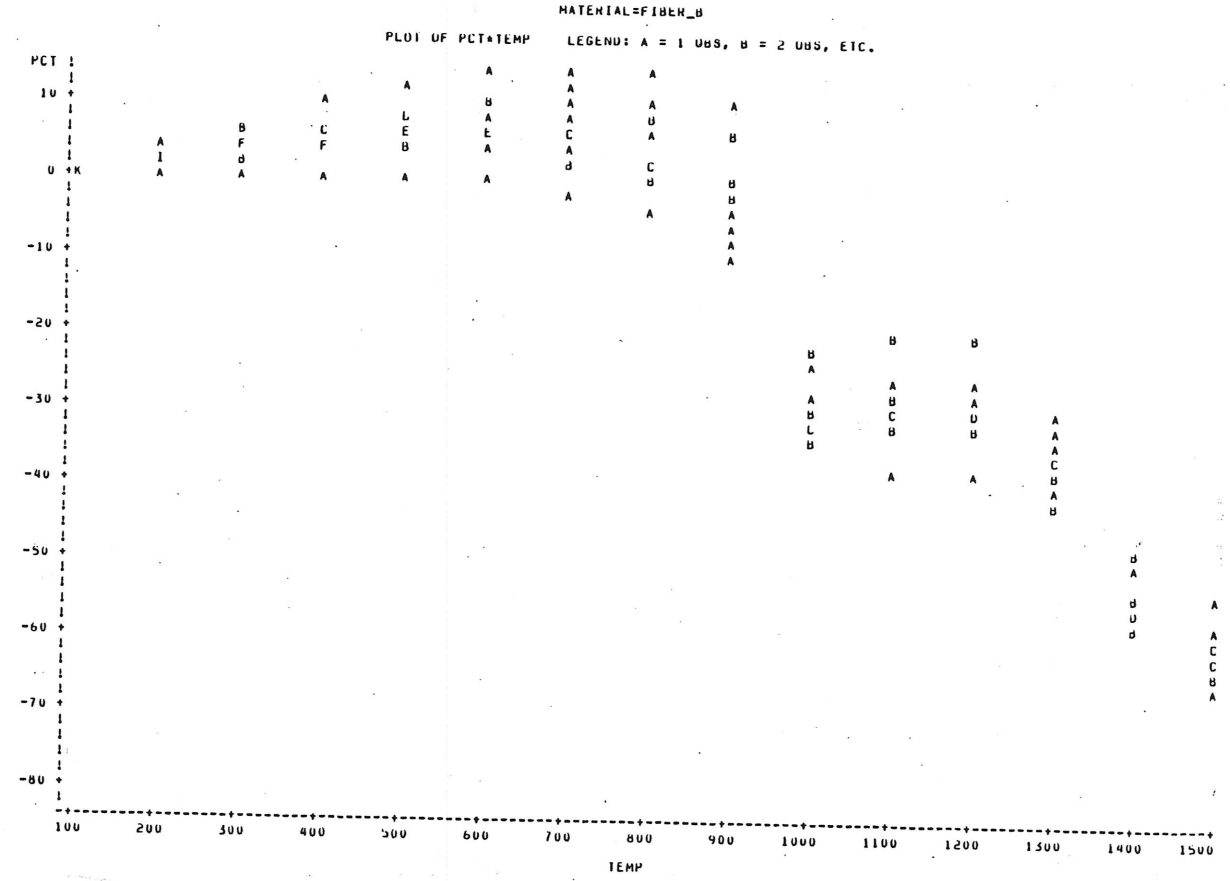

Figure 8

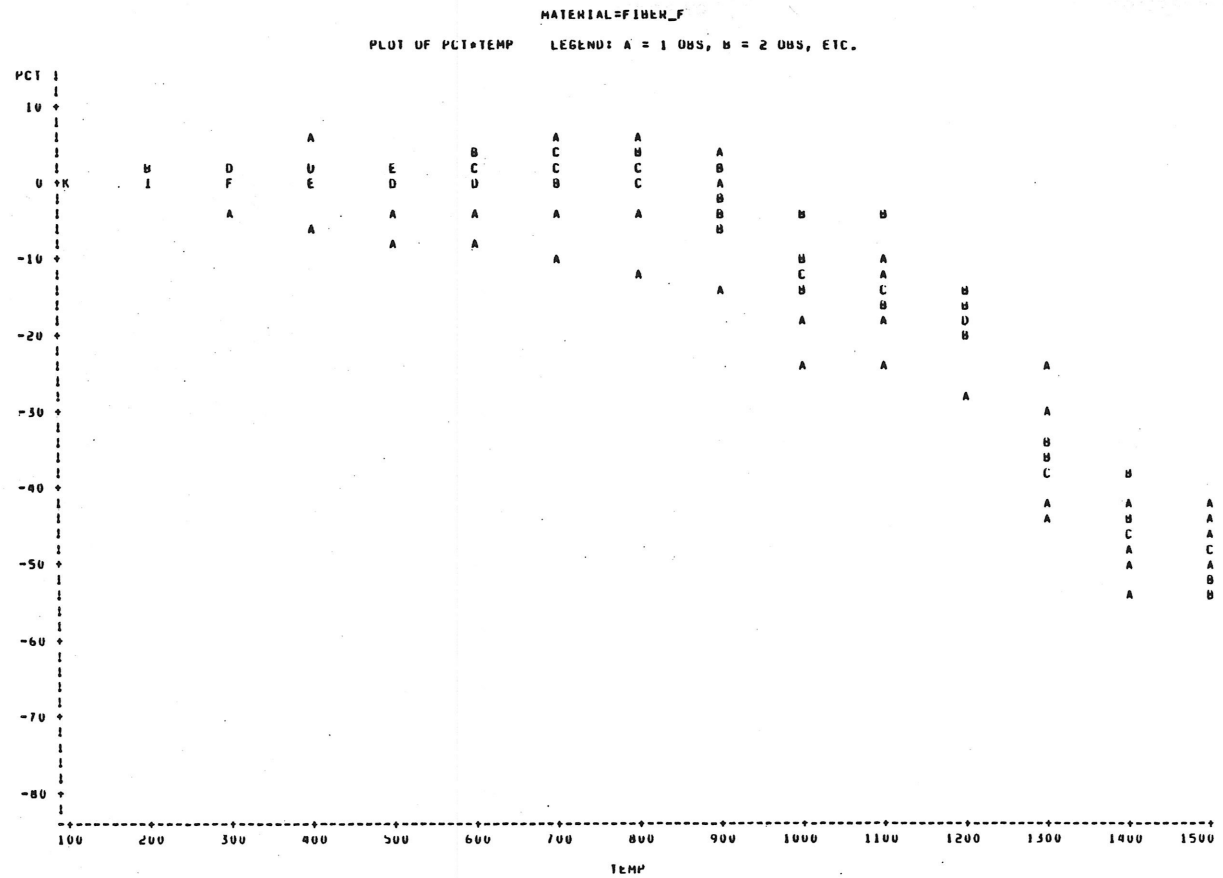

Figure 9

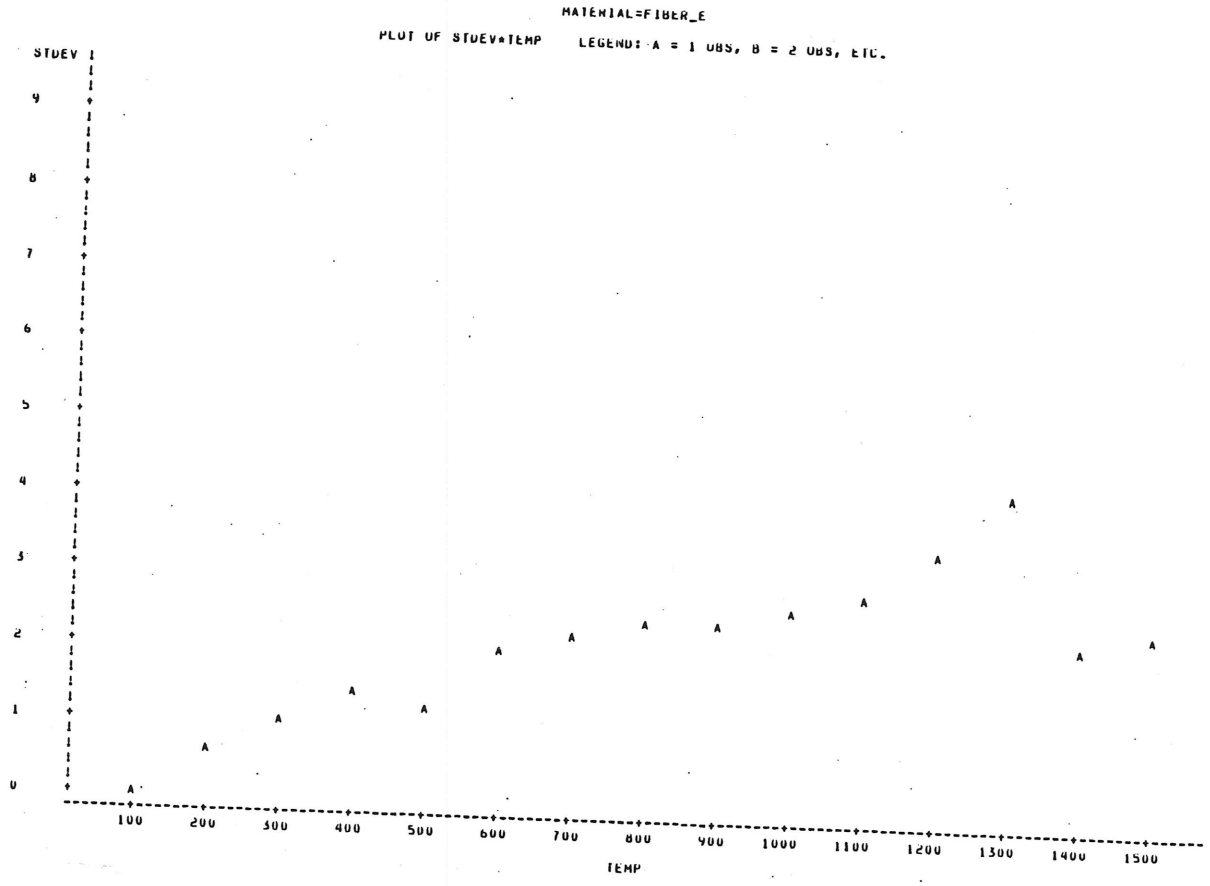

Figure 10

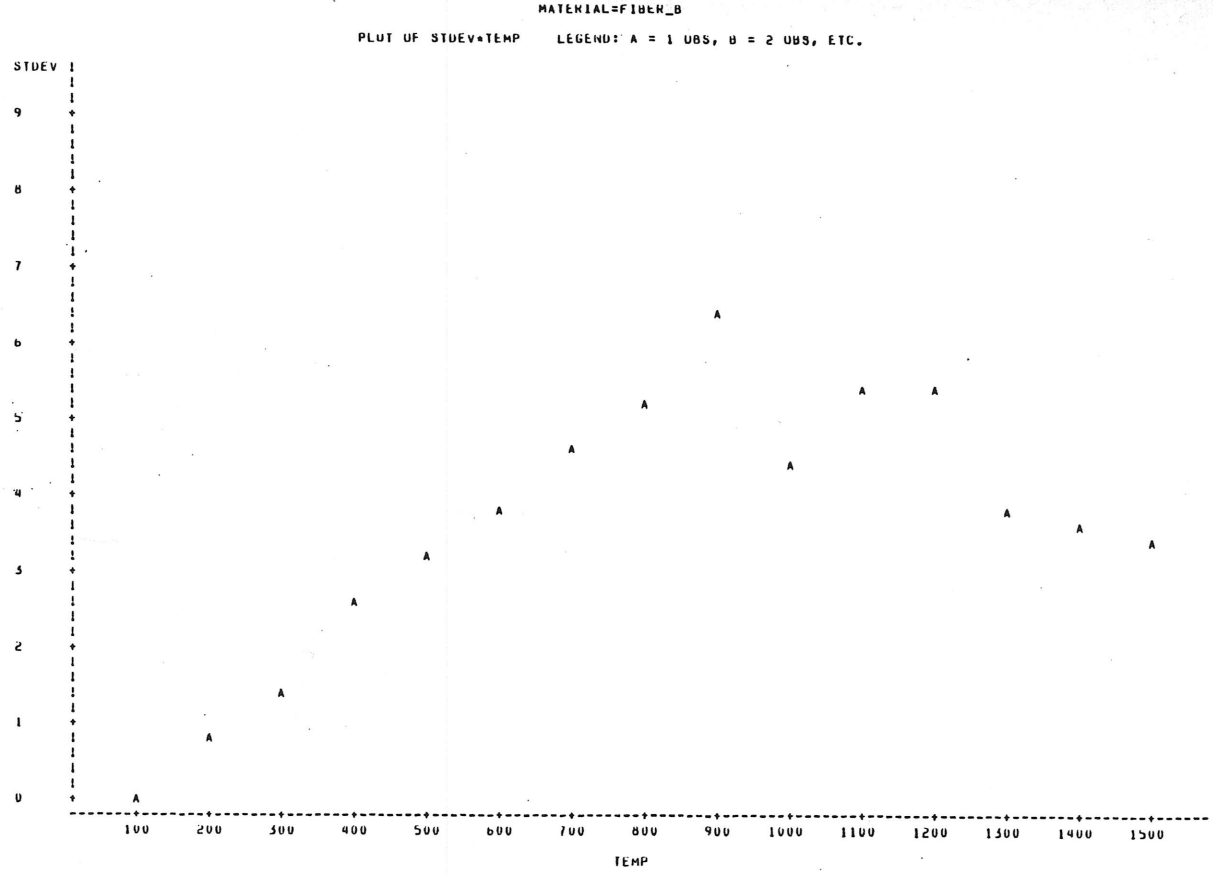

Figure 11

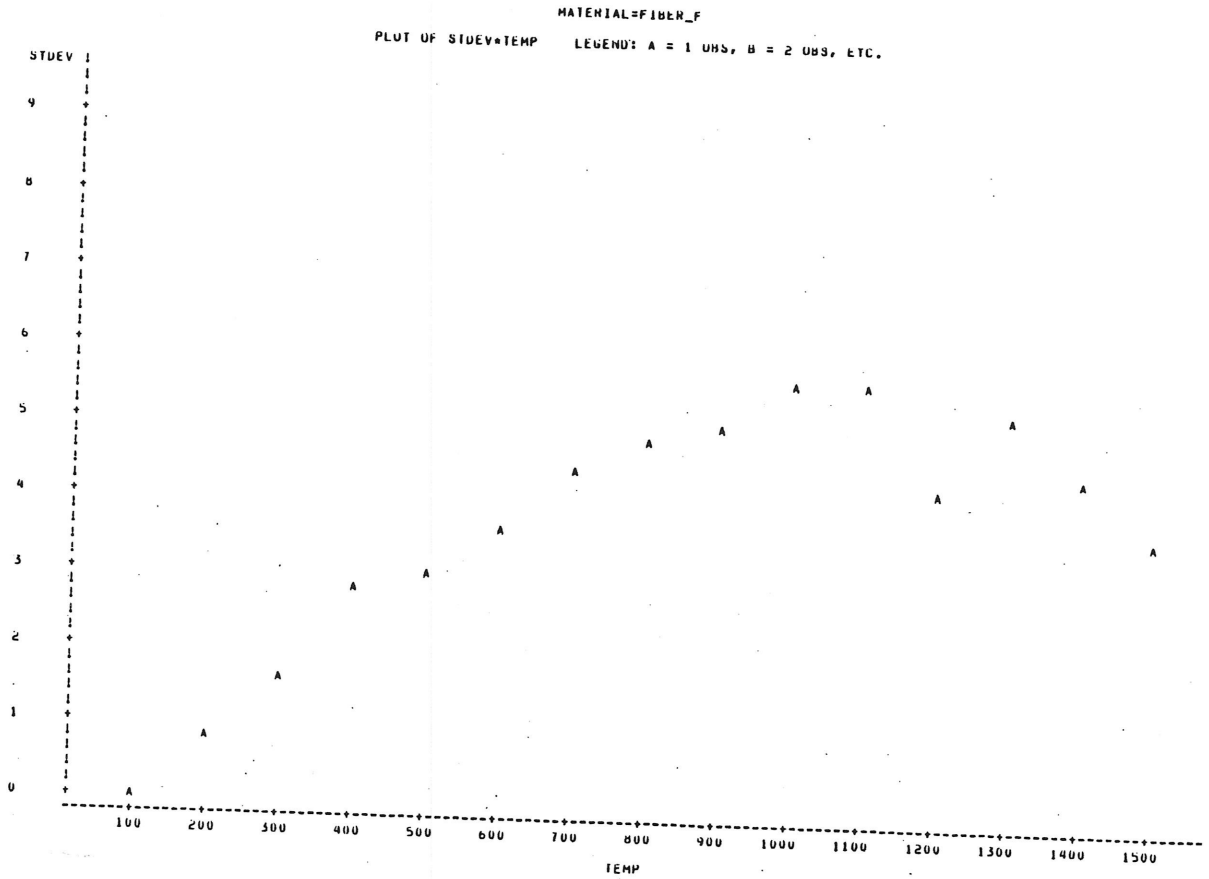

Figure 12

Fig. 13

Mullite formation at 1000°C; Fiber B;

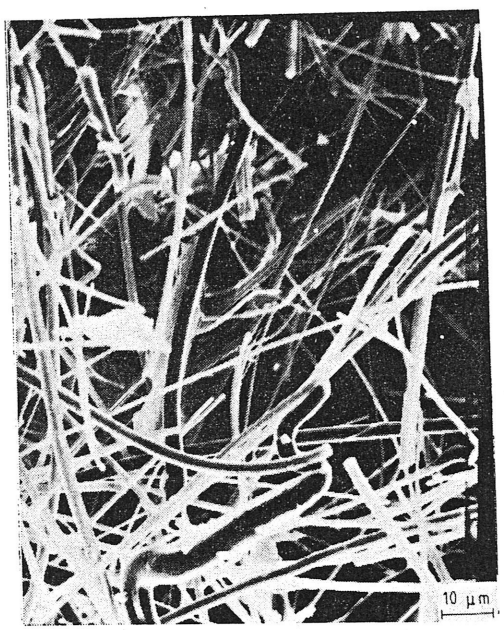

Fig. 14

Mullite formation at 1400°C; Fiber B;

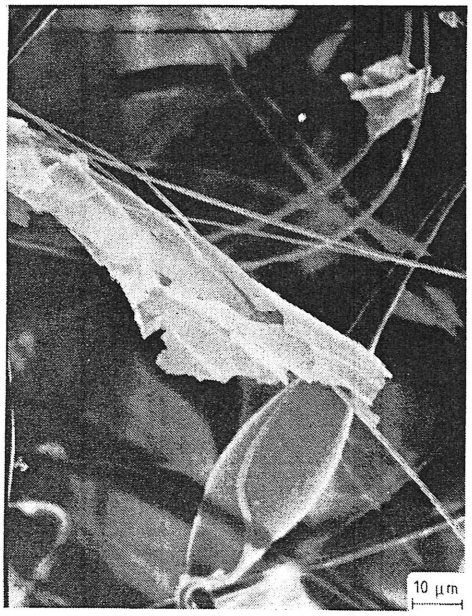

Fig. 15

Fiber Thickening; Fiber B;

Fig. 16

Sheathing of devitrifying fiber; Fiber B;

Fig. 17

Sheathing of devitrifying fiber; Fiber B;

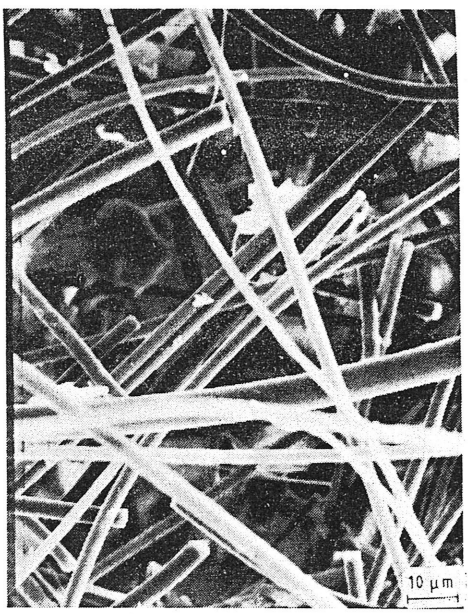

Fig. 18

Mullite formation at 700°C; Fiber E;

Fig. 19

Recrystallization to α -alumina; Fiber E;

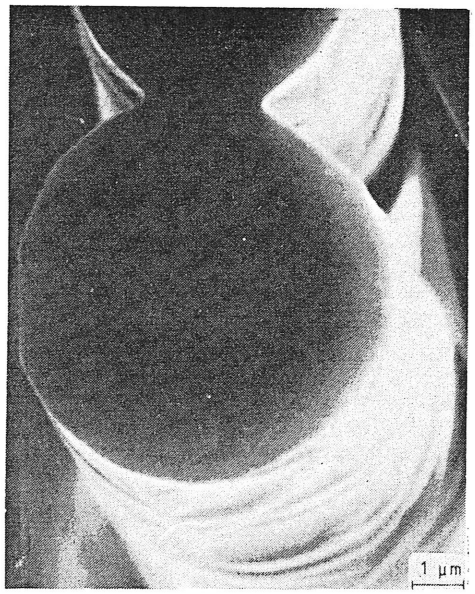

Fig. 20

Recrystallization to α -alumina; Fiber E;

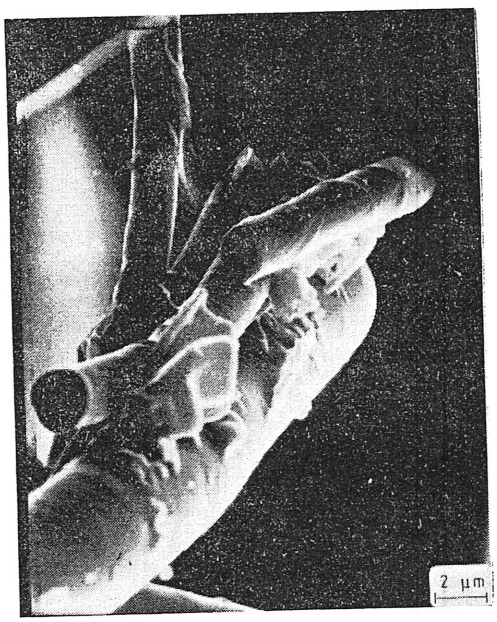

Fig. 21

Fusing of fibers; Fiber E;

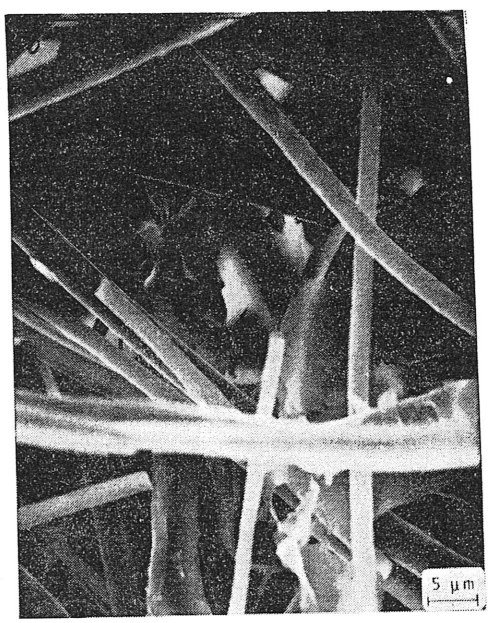

Fig. 22

Mullite formation at 1250°C; Fiber F;

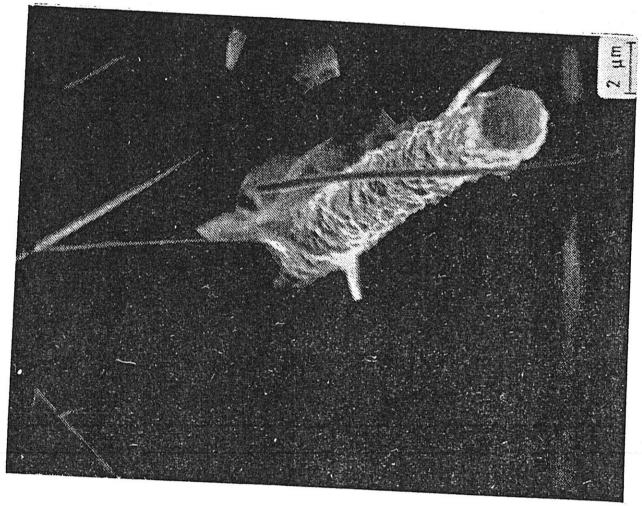

Fig. 23
Cristobalite formation; Fiber F;

P. Dietrichs, W. Krönert, Aachen, Deutschland

EINFLUSS UNTERSCHIEDLICHER GASATMOSPHÄREN AUF KERAMISCHE FASERWERKSTOFFE

1.Einleitung

Steigende Energiekosten führen im Industrieofenbau dazu, in zunehmendem Maße feuerfeste Zustellungen in Leichtbautechnik mit wärmedämmenden Baustoffen auszuführen, die eine möglichst geringe Wärmeleitfähigkeit in weiten Temperaturbereichen und eine geringe Wärmekapazität aufweisen. Für die Lösung dieser Probleme erscheinen keramische Fasern sowie darauf basierende Faserwerkstoffe mit organischen und anorganischen Bindemitteln geeignet, da sie die zuvor formulierten Anforderungen weitgehend erfüllen. In den letzten Jahren sind diese Werkstoffe zunehmend zur Hochtemperaturisolation in den verschiedensten Industrien eingesetzt worden. In einer Vielzahl von Publikationen berichten Faserhersteller und auch Betreiber der entsprechenden Anlagen über die praktische Bewährung dieser Materialien sowie deren Materialeigenschaften und geeignete Zustellungstechniken (1-16). Die Anwendungsmöglichkeiten keramischer Faserwerkstoffe beschränken sich nicht nur auf Teilbereiche industrieller Ofenanlagen; bestimmte Öfen werden inzwischen komplett mit Fasern zugestellt, so z.B. großvolumige Glühöfen (17-26). Diese Materialien können je nach chemischer Zusammensetzung bis zu Temperaturen von 1500^{o}C bzw. 1600^{o}C (Kurzzeitanwendung) eingesetzt werden;konventionelle wärmedämmende Baustoffe wie Feuerleichtsteine bis zu